Simplified VERDICT diffusion imaging and modelling for efficient characterisation of prostate cancer

Adam Phipps[1], Natasha Thorley[1], Alistair Lamb[1], Tom Syer[1,2], Eleftheria Panagiotaki[3], Shonit Punwani[1], and David Atkinson[1]
[1]Centre for Medical Imaging, UCL, London, United Kingdom, [2]Department of Radiology, University of Cambridge, Cambridge, United Kingdom, [3]Centre for Medical Image Computing, UCL, London, United Kingdom

Synopsis

Keywords: Microstructure, Prostate

Motivation: VERDICT diffusion imaging and modelling for prostate cancer characterisation requires significant scan time which hinders its clinical practicality.

Goal(s): We aim to reduce the scan time requirement of VERDICT through paired model simplification and acquisition reduction whilst retaining model fitting accuracy and diagnostic performance.

Approach: We evaluated the model fitting accuracy and diagnostic performance of three simplified VERDICT schemes on 97 patients who underwent targeted biopsy.

Results: Our results demonstrate that a scan time reduction of ≈30% can be achieved with minimal impact to performance; model parameters were recovered with <5% mean bias and no significant change in diagnostic performance was observed.

Impact: Reducing the scan time of VERDICT diffusion imaging could help to enable integration of VERDICT into clinical practice which could help to reduce the number of healthy men referred for biopsy.

Introduction

VERDICT diffusion imaging utilises a three compartment model of prostate tissue microstructure to characterise lesions of prostate cancer (PCa)[1,2]. The intracellular volume fraction (f_{IC}) found through model fitting has demonstrated superior ability to distinguish cases of clinically significant cancer compared to conventionally used ADC[3]. Addition of VERDICT to routine multiparametric MRI (mpMRI) could allow improved characterisation of suspicious lesions and could help to reduce the number of healthy men referred for biopsy.

Image acquisition for the current VERDICT scheme consists of five diffusion images (b=90-3000 s/mm^2) with combined scan time of 12 minutes. For integration with routine mpMRI, the scan time of VERDICT needs reduction. The b=3000 scan takes 3:25 min and has the lowest SNR so is a good candidate for removal. Further, model simplification may enable more robust fitting with fewer scans so could aid efficiency improvement. The vascular component of prostate tissue is small and predicted vascular signal is only appreciable for b≲250 [4]. Thus, scans with b≥250 should be well described by the extracellular (EES) and intracellular (IC) compartments; model simplification could be sensibly achieved through simultaneous removal of the vascular compartment and the b=90 scan (0:40 min).

In this work, we evaluate the impact of model simplification and acquisition reduction on the fitting and diagnostic performance of f_{IC}.

Materials and Methods

This work utilises in vivo VERDICT imaging, mpMRI reporting, and biopsy results from the INNOVATE clinical trial[5] (NCT02689271). A subset (N=97/165) of the biopsied cohort was analysed with near equal split of biopsy result (47 positive vs 50 negative). Lesions of PCa with Gleason grade 3+4 or higher were classified as clinically significant (positive biopsy).

Three simplified VERDICT schemes were evaluated retrospectively and compared to the current VERDICT scheme (orig). Scheme simplifications were: (1) exclusion of b3000 scan (ex3000); (2) removal of b90 scan and vascular compartment (noVASC); and (3) both (1) and (2) (noVASCex3000). The VERDICT-AMICO framework was implemented for model fitting[6].

The f_{IC} fitting performance of each simplified scheme was first evaluated through simulation. Diffusion signal was simulated for 200 voxels with randomised tissue parameters (f_{IC}=[0.2,0.9], f_{VASC}=[0.0,0.3], f_{EES}=1-f_{IC}-f_{VASC}, 100 random cell radii R=[0.1,15.1]). For each voxel, fIC fitting bias and variance was evaluated over 200 Rician noise instances (b=0 SNR 20).

To evaluate in vivo performance, regions of interest (ROIs) were drawn around suspicious lesions from mpMRI reporting (TS). ROIs were transferred to the b=0 image acquired with the b3000 image and edited to account for distortion differences and patient motion (NT). This image was used as the registration target during processing so aligns with output f_{IC} maps. For an unbiased comparison of schemes, ROIs were drawn and edited blind to f_{IC} maps. A quantitative comparison of median lesion f_{IC} and diagnostic performance was conducted between schemes.

Results and Discussion

Figure 1 displays the results from simulation; notably, a reduced fitting variance is observed for 'noVASC' which indicates improved robustness to noise. The fitting variances of 'orig' and 'noVASCex3000' are comparable. A small positive bias is observed for f_{IC}s from 'noVASC' and 'noVASCex3000'; however, these biases are small compared to the corresponding f_{IC} fitting standard deviations and are largely independent of the simulated vascular volume fraction. Figure 3 illustrates that the in vivo f_{IC} biases between schemes are small and consistent with simulation results (mean bias <5% of total volume fraction). A qualitative comparison of f_{IC} maps also reveals consistency between schemes (Figure 2). These results indicate good agreement between f_{IC}s calculated from each scheme and suggest vascular signal is predominantly assigned to the extracellular compartment following model simplification.

No significant difference in diagnostic performance is observed between schemes (Table 1, Figure 4). The f_{IC} thresholds and specificities at 90% sensitivity obtained in this work are notably lower than those found in [3]. We speculate that this discrepancy can be primarily attributed to differences in the ROI drawing method used in [3] (unblind to f_{IC}). Further, the current study analysed a subset of patients included in [3] so exact agreement was not expected. The large confidence intervals displayed in Table 1 illustrate high sensitivity to individual data points at this small patient cohort size. Future work will analyse a larger patient cohort, utilise multiple ROI drawers, and experiment with f_{IC}-guided ROI drawing.

Conclusions

Our results indicate that both model simplification through removal of the vascular compartment and acquisition reduction through exclusion of b=90 and b=3000 scans have minimal impact on fIC fitting and diagnostic performance. These scheme simplifications offer a ≈30% reduction in scan time and could help to enable efficient integration of VERDICT imaging into routine mpMRI.

Acknowledgements

EPSRC Centre for Doctoral Training i4Health (EP/S021930/1)

The INNOVATE study: Prostate Cancer UK (PG14-018-TR2)

References

1. Panagiotaki E, Walker-Samuel S, Siow B, et al. Noninvasive quantification of solid tumor microstructure using VERDICT MRI. Cancer Res. 2014;74(7):1902-1912. doi:10.1158/0008-5472.CAN-13-2511

2. Panagiotaki E, Chan RW, Dikaios N, et al. Microstructural Characterization of Normal and Malignant Human Prostate Tissue With Vascular, Extracellular, and Restricted Diffusion for Cytometry in Tumours Magnetic Resonance Imaging. Invest Radiol. 2015;50(4). doi: 10.1097/RLI.0000000000000115

3. Singh S, Rogers H, Kanber B, et al. Avoiding Unnecessary Biopsy after Multiparametric Prostate MRI with VERDICT Analysis: The INNOVATE Study. Radiology. 2022;305(3):623-630. doi:10.1148/radiol.212536

4. Le Bihan D. What can we see with IVIM MRI? Neuroimage. 2019;187:56-67. doi:10.1016/j.neuroimage.2017.12.062

5. Johnston E, Pye H, Bonet-Carne E, et al. INNOVATE: A prospective cohort study combining serum and urinary biomarkers with novel diffusion-weighted magnetic resonance imaging for the prediction and characterization of prostate cancer. BMC Cancer. 2016;16(1):816. doi:10.1186/s12885-016-2856-2

6. Bonet-Carne E, Johnston E, Daducci A, et al. VERDICT-AMICO: Ultrafast fitting algorithm for non-invasive prostate microstructure characterization. NMR Biomed. 2019;32(1). doi:10.1002/nbm.4019

Figures

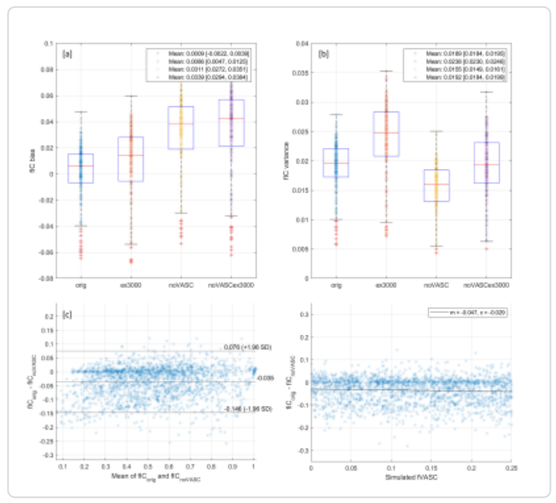

Figure 1: Simulation results for f_{IC} fitting performance. Subfigures [a] and [b] display the bias and variance of fIC fitting from each scheme. Distribution means and 95% confidence intervals are displayed in the legend. Subfigure [c] displays a Bland Altman plot comparing f_{IC} values obtained from the 'orig' and 'noVASC' schemes; subfigure [d] illustrates how the agreement of f_{IC} values obtained from these schemes depends on the simulated vascular volume fraction. The line of best fit with gradient 'm' and intercept 'c' is displayed.

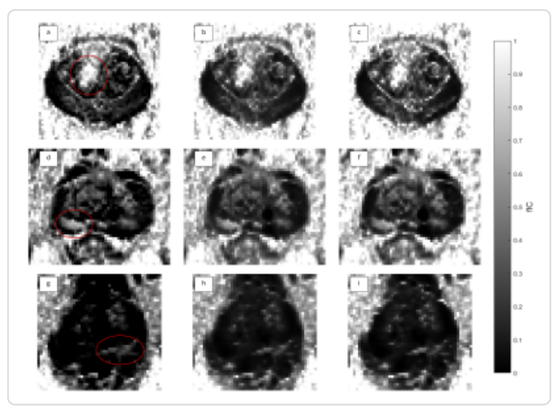

Figure 2: Example f_{IC} image slices displayed in grayscale [0, 1]. Columns [a]-[g], [b]-[h], and [c]-[i] are from schemes 'orig', 'noVASC', and 'noVASCex3000' respectively. Biopsy results are Gleason 5+4 for row [a]-[c], Gleason 3+4 for row [d]-[f], and negative biopsy for row [g]-[i]. Red ellipses outline approximate location of suspicious lesions from mpMRI.

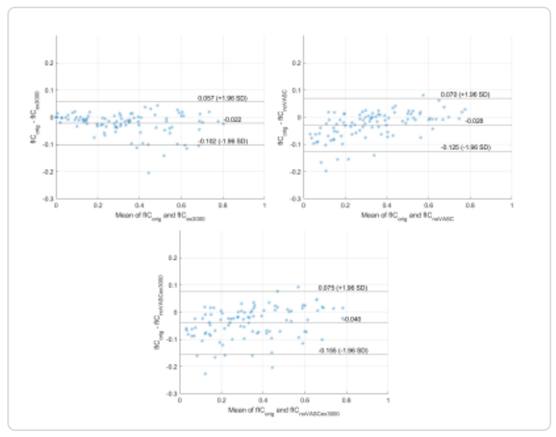

Figure 3: Bland Altman plots displaying agreement of median lesion f_{IC}s calculated from each VERDICT scheme. Mean biases and 95% confidence intervals: 'ex3000' -0.022 [-0.030,-0.014]; 'noVASC' -0.028 [-0.038, -0.018]; 'noVASCex3000' -0.040 [-0.052,-0.028].

Scheme	Compartments	Excluded Scans	ROC AUC	Sensitivity	Threshold	Specificity
orig	IC, EES, VASC	None	0.834 [0.729, 0.906]	0.9 [0.870, 0.928]	0.232 [0.082, 0.282]	0.620 [0.122, 0.755]
ex3000	IC, EES, VASC	3000	0.809 [0.703, 0.877]	0.9 [0.872, 0.927]	0.231 [0.063, 0.297]	0.520 [0.157, 0.720]
noVASC	IC, EES	90	0.849 [0.755, 0.915]	0.9 [0.870, 0.929]	0.264 [0.157, 0.306]	0.580 [0.185, 0.796]
noVASCex3000	IC, EES	90, 3000	0.821 [0.727, 0.891]	0.9 [0.872, 0.927]	0.249 [0.163, 0.319]	0.480 [0.244, 0.727]

Table 1: Diagnostic performance of VERDICT schemes, measured using area under receiver operating characteristic curve (ROC AUC), f_{IC} thresholds and specificities are quoted for a sensitivity set at 90%. 95% confidence intervals in sensitivity, ROC AUC, specificity, and threshold found through bootstrapping (Nboot = 10000).

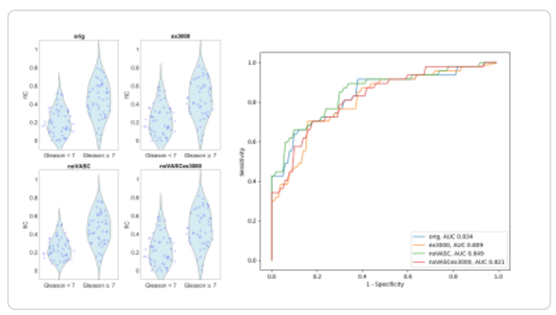

Figure 4: Diagnostic performance of simplified VERDICT schemes. The left subfigures display the distributions of f_{IC}s from each scheme separated by biopsy result. The right subfigure displays the ROC curve for each scheme.